Clinical and Experimental Obstetrics & Gynecology

Clin. Exp. Obstet. Gynecol. **2026**; 53(2): 46464
https://doi.org/10.31083/CEOG46464

Original Research

Mitofusin 2 Attenuates Adenomyosis Progression by Suppressing Epithelial-Mesenchymal Transition: Evidence From Clinical and Experimental Models

Xuan Wang[1], Qing Han[1], Xin Qin[2], Nana Xu[3], Chun Ding[1], Hong Ye[1,*]

[1]The First College of Clinical Medical Science, China Three Gorges University, Yichang Central People's Hospital, 443003 Yichang, Hubei, China
[2]Department of Pathology, The Fifth People's Hospital of Yichang, 443007 Yichang, Hubei, China
[3]Department of Ultrasound, The Fifth People's Hospital of Yichang, 443007 Yichang, Hubei, China
*Correspondence: yehong15586376231@126.com (Hong Ye)
Academic Editor: Michael H. Dahan
Submitted: 10 September 2025 Revised: 19 October 2025 Accepted: 13 November 2025 Published: 4 February 2026

Abstract

Background: Adenomyosis involves epithelial-mesenchymal transition (EMT), yet the role of mitochondrial regulator Mitofusin 2 (Mfn2) remains unclear. This study investigated the role of Mfn2 in adenomyosis-related EMT and evaluated its potential as a therapeutic target. **Methods**: Mfn2 expression was compared between human adenomyotic and normal endometrial tissues using immunohistochemistry. Transforming growth factor-beta 1 (TGF-β1)-induced EMT was established in Ishikawa cells, and Mfn2 was overexpressed to assess EMT markers using quantitative polymerase chain reaction (qPCR) and Western blot, as well as cell migration and invasion (via scratch and Transwell assays). A neonatal mouse model of tamoxifen-induced adenomyosis received intrauterine lentiviral Mfn2 overexpression. Uterine morphology, fibrosis, and EMT markers were evaluated after 20 days. **Results**: Mfn2 was significantly downregulated in adenomyosis ($p < 0.05$). Overexpression of Mfn2 reversed EMT, evidenced by increased E-cadherin and decreased N-cadherin and Vimentin ($p < 0.05$), suppressed cell migration and invasion *in vitro* ($p < 0.05$), improved uterine morphology ($p < 0.05$), reduced fibrosis ($p < 0.05$), and inhibited EMT *in vivo*. **Conclusion**: Mfn2 suppresses EMT in adenomyosis, suggesting its protective role and potential as a therapeutic target.

Keywords: adenomyosis; epithelial-mesenchymal transition (EMT); Mitofusin 2 (Mfn2); transforming growth factor-beta 1 (TGF-β1)

1. Introduction

Adenomyosis (ADS) is a common gynecological disease, and the main pathological feature is ectopic growth of endometrial glands and stroma into the myometrium [1]. The ectopic growth results in a cascade of clinical problems, including dysmenorrhea, dyspareunia, abnormal uterine bleeding, and infertility [2,3], which seriously impair the quality of life of reproductive-age women [1]. The estimated prevalence of adenomyosis in women of reproductive age ranges from 20% to 34.6% on the basis of radiographic assessment to 10% to 88% on the basis of pathological diagnosis in resected uterine specimens, so this diagnostic heterogeneity underscores the underrecognition of this disease [4].

It has been demonstrated by recent studies that endometrial basal cell abnormal proliferation and invasion have intimate connections with epithelial-mesenchymal transition (EMT) [5]. EMT is a salient biological program: through reprogramming of some molecules, epithelial cells are able to transform into extremely migratory and invasive mesenchymal cells. Despite the inevitability of the process in embryonic development and tissue restoration, its pathological activation is widely implicated in inflammatory reactions and metastasis of tumors [6,7]. In adenomyosis, EMT may lead to the phenotypic transformation of endometrial epithelial cells, which lose their original features step by step, acquire invasive stromal cell characteristics, and further breach the basal barrier and invade the myometrium to form the typical ADS lesions [8].

Because the dynamic equilibrium of mitochondria is in charge of cell homeostasis and even the body's homeostasis, as the core center of cellular energy metabolism, the dynamic equilibrium of mitochondria is thus very crucial. In the regulating network, Mitofusin 2 (Mfn2) is also the core executor of mitochondrial fusion and an important safeguard of mitochondrial network structure [9]. By interacting with Mitofusin 1 (Mfn1) and other proteins to form functional complexes, Mfn2 initiates processes of membrane fusion between the mitochondria [10], thus ensuring mitochondrial function and morphology integrity. The regulation has a profound effect on basic processes such as energy metabolism, signaling by calcium, and cell life and death processes [11–13]. It should be noted that the abnormal expression or dysfunction of Mfn2 has been demonstrated to be closely related to a series of severe diseases, ranging from neurodegenerative diseases, metabolic disorders, to cardiovascular diseases, and even throughout the whole process of tumor occurrence, development, and metastasis [14–17].

With an increasing depth of research on cell biology and molecular mechanisms, the regulatory network between Mfn2 and EMT has been progressively exposed. Present data suggest that Mfn2 has a tumor suppressor function by dynamically regulating the balance of mitochondrial fusion/fission in thyroid cancer progression and directly regulates the EMT process [18]. In ovarian cancer xenograft models, Mfn2 may be induced by genetic or drug approaches to cause mitochondrial fusion, which strongly inhibits the growth, migration, invasion and EMT phenotype of cancer cells by reducing the level of reactive oxygen species (ROS) [19]—the mechanism is mitochondrial fusion-mediated F-actin remodeling, decreasing the formation of lamella pseudopodia, a key connection in EMT. These findings collectively describe a multi-organ role of Mfn2 as an EMT mediator.

Surprisingly, despite accumulating evidence, the functional role of Mfn2 in ADS remains largely unknown. Based on confirmed Mfn2-EMT regulation in oncology models, and EMT's established role in adenomyosis pathogenesis, we hypothesize that Mfn2 inhibits adenomyosis progression by suppressing EMT in endometrial cells. This study is the first to test this mechanism in benign gynecological disease. By combining the three-dimensional verification system of *in vitro* cell model, clinical sample analysis, and animal experiment, the principal role of Mfn2 in the occurrence and development of diseases will be studied deeply, which will provide a new understanding of ADS pathological mechanism and create the possibility of translational medicine for targeted intervention.

2. Materials and Methods

2.1 Collection of Clinical Samples

In the present study, samples were obtained from the Wujia District of Yichang Central People's Hospital. The experimental group consisted of 15 cases of endometrial tissue of ADS patients, and the control group consisted of 8 cases of endometrial tissue of hysterectomy due to cervical intraepithelial neoplasia. No patients received any hormonal therapy, radiotherapy, or chemotherapy during the last 3 months before surgery. All the specimens were confirmed to be of the proliferative phase by histological examination, and other pathological conditions such as uterine fibroids and endometrial lesions were excluded.

2.2 Cell Culture and Transfection of Plasmid

Given the challenges in primary endometrial epithelial cell isolation and culture stability, we selected the Ishikawa human endometrial adenocarcinoma cell line as a well-established *in vitro* model. Although derived from malignancy, this cell line retains key endometrial epithelial characteristics and is widely used in adenomyosis/endometriosis EMT studies due to its hormone responsiveness and reliable transfection efficiency.

Mycoplasma contamination in the Ishikawa cell line was assessed using PCR and colorimetric assays, with results indicating no contamination. To verify genetic identity and purity, genomic DNA was extracted and amplified using a multiplex PCR system targeting 20 short tandem repeat (STR) loci and a gender identification marker. The amplified products were analyzed using a genetic analyzer and compared against the national database (CCRID, https://http://www.cellresource.cn/) for matching analysis.

The human endometrial cancer cell line Ishikawa (CL-0283, Pricella Biological, Wuhan, Hubei, China) was cultured in DMEM supplemented with 10% FBS and 1% penicillin-streptomycin at 37 °C in 5% CO_2. Cells were divided into four groups: Normal Control, transforming growth factor-beta 1 (TGF-β1) Model, Mfn2 Negative Control (Mfn2-NC), and Mfn2 Overexpression (Mfn2-OE). Cells (1×10^5/well in 6-well plates) were cultured for 24 h, serum-starved for 12 h in DMEM, and then treated: the TGF-β1 Model, Mfn2-NC, and Mfn2-OE groups received 10 ng/mL TGF-β1 (HZ.1011, PeproTech, Rocky Hill, NJ, USA) for 24 h [20]. Mfn2 overexpression plasmid or empty vector plasmid (negative control) was transfected into cells using Lipofectamine 3000 (Invitrogen, Carlsbad, CA, USA) reagent. The plasmid vector sequences are shown in **Supplementary Table 1**. After transfection, the cells were cultured for 24–48 hours and then harvested for further analysis.

2.3 Real-Time Quantitative PCR

Total RNA was extracted using TRIzol. Purified RNA was reverse-transcribed to cDNA using the HiScript III reverse transcription kit (AKR-201, Accuri, Nanjing, Jiangsu, China). Quantitative real-time reverse transcription PCR (qRT-PCR) was performed using ChamQ Universal SYBR quantitative polymerase chain reaction (qPCR) Master Mix (AKR-301, Accuri, Nanjing, Jiangsu, China) on an Agilent Statagene Mx3000P instrument. Primers (Hunan Accuri BioEngineering Co., Ltd., Nanjing, Jiangsu, China) were used. The reaction conditions were: 50 °C for 30 min (reverse transcription); 95 °C for 3 min (pre-denaturation); followed by 40 cycles of 95 °C for 15 sec (denaturation) and 60 °C for 30 sec (annealing). Relative gene expression was calculated using the $2^{-\Delta\Delta Ct}$ method. Primer sequences are provided in **Supplementary Table 2**.

2.4 Western Blot

Proteins were extracted using radioimmunoprecipitation assay (RIPA) lysis buffer (Applygen Technologies Inc., Beijing, China). Protein concentration was determined by bicinchoninic acid (BCA) assay (P0009; PINUOFEI, Beijing, China) and samples were normalized. Samples were mixed with 5× sodium dodecyl sulfate (SDS) loading buffer, denatured by boiling, separated by SDS-polyacrylamide gel electrophoresis (PAGE), and transferred to polyvinylidene fluoride (PVDF) mem-

branes. After blocking with 5% skim milk, membranes were incubated overnight at 4 °C with primary antibodies: E-cadherin (1:20,000, 20874-1-AP; Proteintech, Rocky Hill, NJ, USA), N-cadherin (1:10,000, 22018-1-AP; Proteintech, Rocky Hill, NJ, USA), Vimentin (1:50,000, 10366-1-AP; Proteintech, Rocky Hill, NJ, USA) and Mfn2 (1:2000, CY6638; Abways, Shanghai, China). Following Tris-buffered saline with Tween-20 (TBST) washes, horseradish peroxidase (HRP)-conjugated secondary antibody (1:15,000, G1213; Sevier, Wuhan, Hubei, China) was incubated at room temperature. Proteins were detected using enhanced chemiluminescence (ECL) chemiluminescence and analyzed with Image Lab software (v6.1, Bio-Rad, Hercules, CA, USA).

2.5 Wound Healing Assay

Cell migration was assessed using a scratch wound healing assay. Ishikawa cells (5×10^5 cells/well) were seeded in 6-well plates. Upon reaching ~90–100% confluence, a scratch was created in the monolayer using a sterile pipette tip. Cells were gently washed 3 times with PBS to remove debris and incubated in serum-free DMEM. Images of three random fields per well were captured at 0 h (baseline), 24 h, and 48 h using an inverted microscope. The scratch area at each time point was measured using ImageJ software (v1.53k, NIH, Bethesda, MD, USA). The wound healing rate was calculated as: Healing rate (%) = [1 – (Area at Tn/Area at T_0)] × 100% (Where T_0 = area at 0 h; Tn = area at measurement time point).

2.6 Transwell Invasion Assay

Ishikawa cells (2×10^5 cells/well) were plated in the upper chamber of Matrigel-coated Transwell inserts (BD Biosciences). The lower chamber contained DMEM with 10% FBS. After 48 h incubation at 37 °C/5% CO_2, non-migrated cells in the upper chamber were removed with a cotton swab. Migrated cells on the lower membrane surface were fixed with 4% paraformaldehyde, stained with 0.1% crystal violet, and imaged using an inverted microscope. Invading cells in five random fields per insert were quantified using ImageJ software (v1.53k, NIH, Bethesda, MD, USA); the mean value was calculated and compared statistically.

2.7 Animal Experiments

ICR newborn female mice (<24 h postpartum; Hunan Slake Jingda Laboratory Animal Co., Ltd., China) were housed under SPF conditions (22 ± 2 °C, 50%–60% humidity, 12-h light/dark cycle). Sixty mice were randomly assigned to establish an ADS model using tamoxifen (T5648-1G, Sigma-Aldrich, St. Louis, MO, USA). Model group mice received tamoxifen suspension (1 µg/g in peanut oil/lecithin/purified milk mixture [2:0.2:3 v/v/v]; 5 µL/g) by daily gavage on postnatal days (PND) 2–5 [21]. Controls received the same volume of vehicle without tamoxifen.

At PND 60, three mice per group were sacrificed. Uterine tissues were collected for hematoxylin and eosin H&E staining to confirm successful modeling, defined by histopathological observation of endometrial glands and stroma invading the myometrium to form characteristic adenomyosis lesions, accompanied by significant changes in EMT markers (down-regulated E-cadherin, up-regulated N-cadherin, Vimentin).

After successful modeling, mice were randomly divided into four groups (n = 9/group): Normal Control, ADS Model, Mfn2 Negative Control (LV-NC), and Mfn2 Overexpression (LV-Mfn2). Mice in the LV-NC and LV-Mfn2 groups received intrauterine injections of empty vector lentivirus (LV-NC) or Mfn2-overexpressing lentivirus (LV-Mfn2, 1×10^8 TU/mL; China Jima Gene Co., Ltd., Shanghai, China), respectively [22]. Mice were sacrificed 20 days post-injection, and uterine tissues were collected for analysis. All mice were anesthetized by intraperitoneal injection of 3% sodium pentobarbital (100 mg/kg) before surgery. At the end of the experiment, after anesthesia using the method described above, rapid cervical dislocation was implemented to ensure that the mice had no pain perception.

2.8 H&E Staining

Uterine tissues were fixed in 4% paraformaldehyde (24 h), dehydrated, cleared, paraffin-embedded, and sectioned (5 µm). Sections were dried (60 °C, 2 h), deparaffinized in xylene I and II, and hydrated through graded ethanol (100%, 95%, 80%, 70%). After H&E staining, sections were dehydrated (70%, 80%, 95%, 100% ethanol), cleared in xylene, and mounted with neutral gum. Five random fields per section were imaged under a light microscope.

2.9 Masson Staining

Following hematoxylin and eosin (HE) staining, tissue sections underwent deparaffinization and hydration. Masson's trichrome staining was performed sequentially with: Weigert's iron hematoxylin, ponceau acid fuchsin, differentiation in 1% phosphomolybdic acid, and aniline blue. After dehydration and mounting, collagen fibers (blue) and muscle fibers (red) were visualized under a light microscope. Fiji ImageJ software was used to quantify the percentage of collagen fiber area (5 random fields/section). Collagen regions (stained blue) were identified by Red–Green–Blue (RGB) threshold segmentation (threshold range: blue channel 60–255), and nuclei (dark blue, saturation >90%) and non-specific staining were excluded. The collagen-positive area was calculated as a percentage of the total visual field area.

2.10 Immunohistochemistry

Paraffin-embedded tissue sections (5 µm) were fixed and subjected to H&E staining following standard protocol. For immunohistochemistry (IHC), sections underwent microwave antigen retrieval in 0.01 M sodium citrate buffer (pH 6.0), followed by endogenous peroxidase blocking with 3% H_2O_2. After blocking with 5% BSA, sections were incubated overnight at 4 °C with primary antibody: Mfn2 (1:1200, 12186-1-AP; Proteintech). After PBS washes, sections were incubated with HRP-conjugated secondary antibodies (1:500, G1213; Sevier) at room temperature, developed with 3,3'-diaminobenzidine (DAB), and counterstained with hematoxylin. Sections were then dehydrated, cleared, mounted, and imaged under a light microscope (5 random fields/section). Mfn2-positive area percentage and expression levels were quantified using ImageJ software.

2.11 Statistical Analysis

Statistical analysis was performed with GraphPad Prism software (version 8.0, San Diego, CA, USA). Continuous data are presented as mean ± standard deviation (SD). Two-group comparisons were performed using either the unpaired Student's *t*-test or the Mann-Whitney U test, as appropriate based on data distribution and normality assumptions. Comparisons between more than two groups were performed using one-way analysis of variance (ANOVA) followed by Tukey's post-hoc test for pair-wise comparisons. Statistical significance was a *p*-value of <0.05. All experiments were conducted with a minimum of three independent biological replicates.

3. Results

We found that Mfn2 protein levels were significantly lower in the endometrium of adenomyosis patients compared to healthy women. This hints that Mfn2 might be involved in the disease. Looking closer at a process called EMT—which is important in diseases like this—we saw changes in key markers: the "epithelial" marker E-cadherin (both mRNA and protein) was down ($p < 0.05$), while the "mesenchymal" marker N-cadherin, Vimentin was up ($p < 0.05$). This confirms EMT is happening in adenomyosis. Since Mfn2 was low at the same time, we suspected its decrease might be linked to triggering EMT (Fig. 1).

To test this link, we used a lab model of EMT (treating Ishikawa cells with TGF-β1). Just like in patients, Mfn2 levels dropped significantly in these treated cells ($p < 0.05$). The EMT markers also changed as expected: E-cadherin down ($p < 0.05$), N-cadherin and Vimentin up ($p < 0.05$). Importantly, these cells became much better at moving and invading ($p < 0.05$)—classic signs of EMT. Then, we boosted Mfn2 levels in this model. This successfully reversed the EMT changes: E-cadherin increased ($p < 0.05$), N-cadherin and Vimentin decreased ($p < 0.05$). Crucially, it also significantly reduced the enhanced cell migration and invasion caused by TGF-β1 ($p < 0.05$). This strongly suggests Mfn2 acts like a brake, slowing down EMT and the invasive cell behavior seen in adenomyosis (Figs. 2,3).

To see if Mfn2 protects against adenomyosis in a living system, we used a mouse model of the disease. Mice with adenomyosis showed the expected problems: disrupted boundary between the endometrium and muscle layer, glands invading the muscle, and increased fibrosis ($p < 0.05$). Giving these mice a control virus (LV-NC) didn't help. However, using a virus to increase Mfn2 levels (LV-Mfn2) in the uterus significantly improved things: the tissue boundary was less disrupted, gland invasion was reduced, and fibrosis was lessened ($p < 0.05$). We confirmed Mfn2 levels were indeed higher in the treated mice ($p < 0.05$). Just like in the cells and patients, the diseased mice showed EMT activation (low E-cadherin ($p < 0.05$), high N-cadherin, Vimentin) ($p < 0.05$). Boosting Mfn2 reversed these EMT marker changes too (Figs. 4,5).

Together, our results show Mfn2 levels are consistently low in adenomyosis across different systems. Increasing Mfn2 counteracts the EMT process, reduces the invasive potential of endometrial cells, and significantly improves disease features in mice. This strongly indicates that Mfn2 plays a protective role in adenomyosis by inhibiting EMT, making it a promising potential target for treatment.

4. Discussion

This study provides the first evidence that Mfn2 critically inhibits adenomyosis progression by suppressing EMT. Through integrated clinical, cellular, and animal analyses, we consistently demonstrated significant Mfn2 downregulation in adenomyosis endometrium, which strongly correlated with aberrant EMT activation (↓ E-cadherin/↑ N-cadherin, ↑ Vimentin). Mechanistically, Mfn2 overexpression in TGF-β1-stimulated Ishikawa cells reversed EMT-driven cell invasion, while *in vivo* lentiviral delivery of Mfn2 restored uterine architecture and reduced fibrosis in tamoxifen-induced adenomyosis mice. Critically, unlike tumors, adenomyosis has no malignant transformation; thus, the anti-EMT effect of Mfn2 is primarily directed against tissue invasion and fibrosis rather than metastasis. This aligns with its documented role in suppressing pathological fibrosis in other organs, establishing Mfn2 as a novel therapeutic target for this benign gynecological disorder.

Taken together with our findings, we propose a comprehensive hypothesis that Mfn2 may suppress ROS burst and reverse pathological metabolic reprogramming by inhibiting mitochondrial homeostasis (fusion/fission), ultimately inhibiting EMT. The basic mechanism may include the following interrelated levels:

1. Regulation of mitochondrial morphology and function: as a key regulatory protein of mitochondrial outer membrane fusion, down-regulation of Mfn2 expression di-

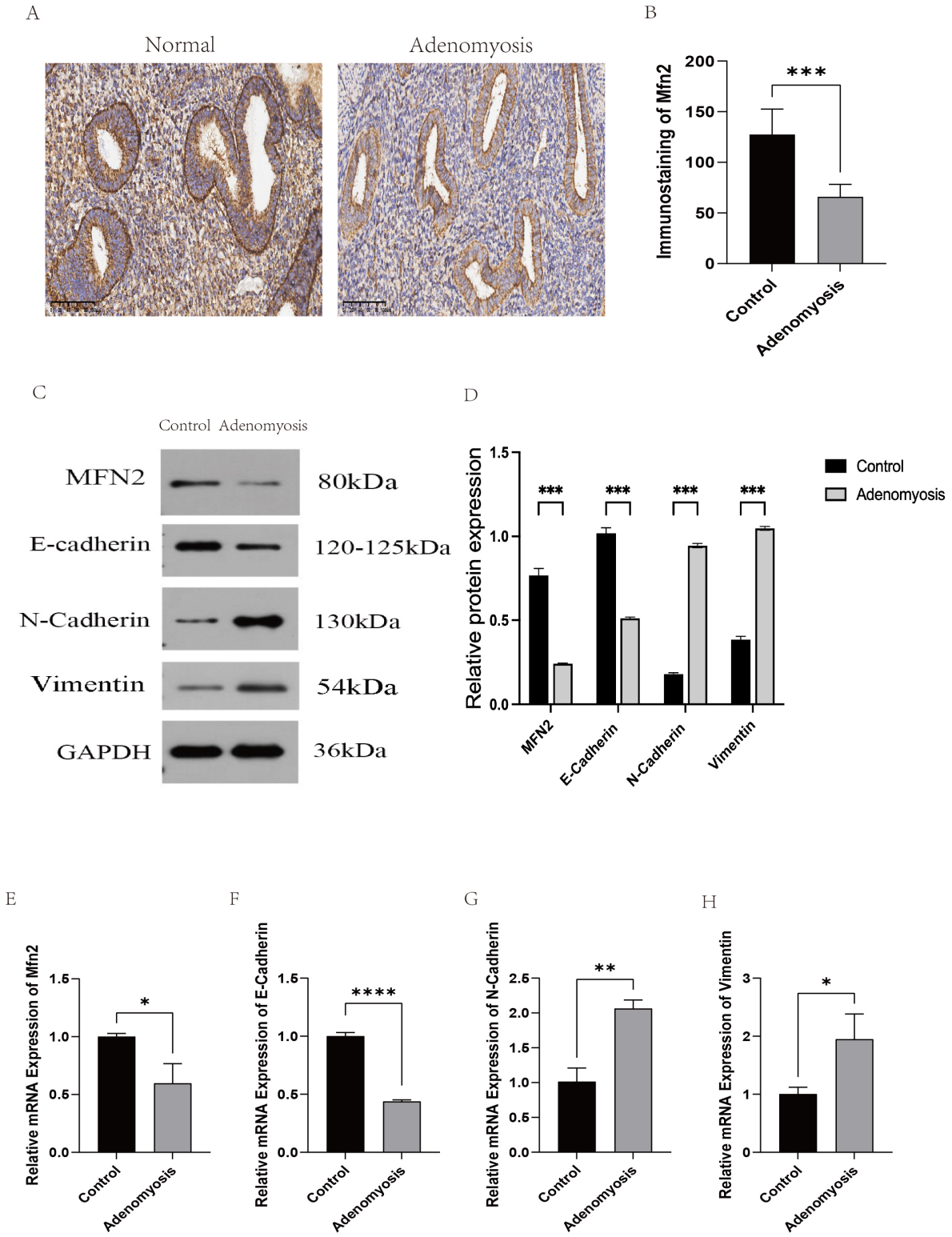

Fig. 1. Immunohistochemical, Western Blot, and qPCR results of clinical samples. (A,B) Immunohistochemistry was used to compare the expression of Mfn2 in normal endometrium and adenomyosis endometrium. Scale bar: 100 μm (×200). (C,D) Western Blot was used to detect the protein expression of E-cadherin, N-cadherin, Vimentin, and Mfn2 in the endometrium of the two groups. (E–H) qPCR was used to detect the expression of E-cadherin, N-cadherin, Vimentin, and Mfn2 mRNA in the two groups. Values represent mean ± SD, Adenomyosis group n = 15, Control group n = 8 (*t*-test). *$p < 0.05$, **$p < 0.01$, ***$p < 0.001$, ****$p < 0.0001$. qPCR, quantitative polymerase chain reaction; Mfn2, Mitofusin 2; SD, standard deviation.

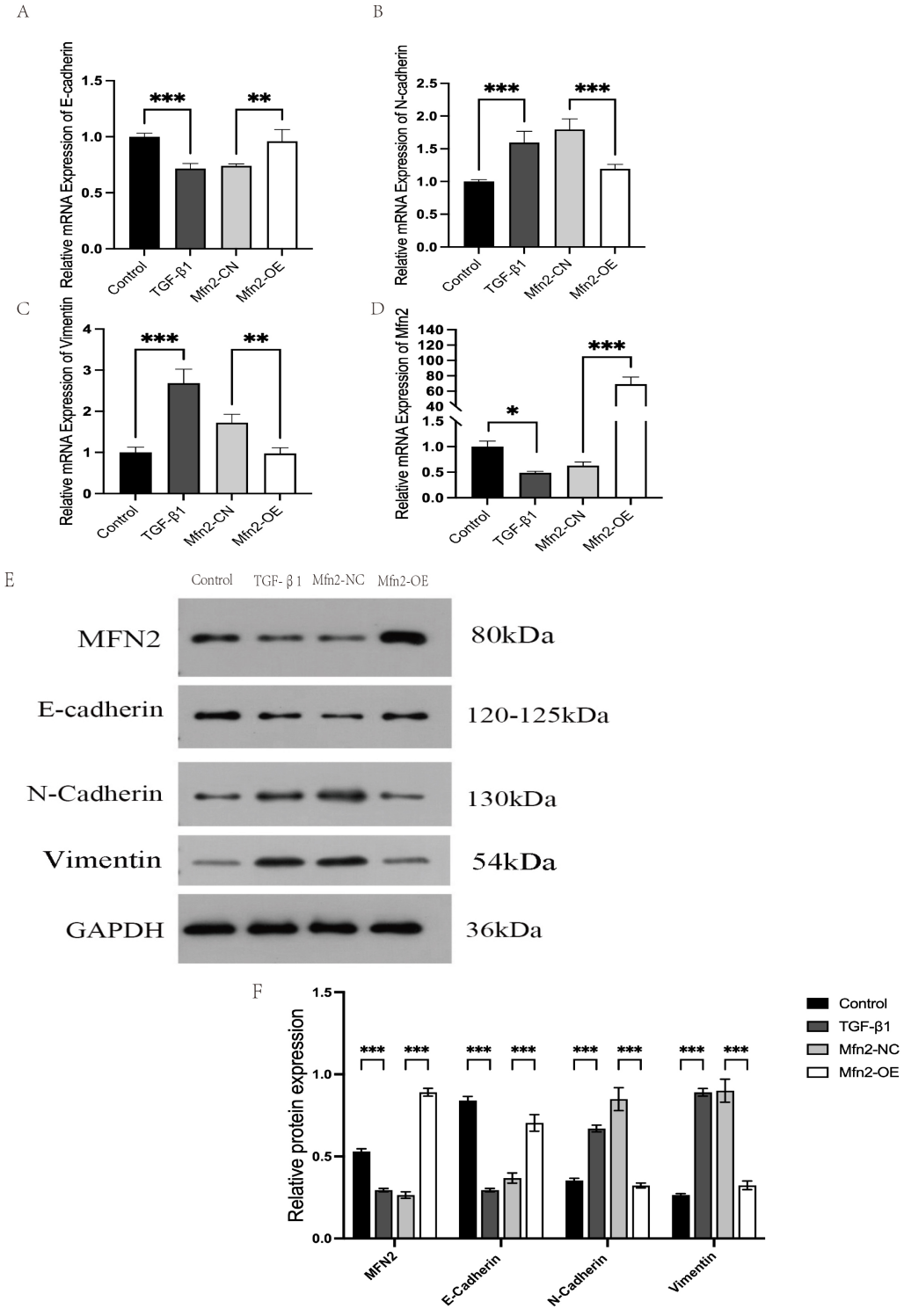

Fig. 2. Ishikawa cells were treated with TGF-β1 to induce EMT model and the expression levels of each factor were detected by qPCR and Western Blot after plasmid transfection. The Mfn2 negative control plasmid was represented by Mfn2-NC. The Mfn2 overexpression plasmid was represented by Mfn2-OE. (A–D) qPCR was used to detect the mRNA expressions of E-cadherin, N-cadherin, Vimentin and Mfn2 in the control group, TGF-β1 model group, Mfn2-NC group and Mfn2-OE group. Values represent mean $\pm$ SD, n = 3 (ANOVA). (E,F) Western Blot was used to detect the protein expression of E-cadherin, N-cadherin, Vimentin and Mfn2 in the control group vs the TGF-β1 model group and the Mfn2 negative control group (Mfn2-NC) vs the Mfn2 overexpression group (Mfn2-OE). Values represent mean $\pm$ SD, n = 3 (ANOVA). *$p < 0.05$, **$p < 0.01$, ***$p < 0.001$. TGF-β1, transforming growth factor-beta 1; EMT, epithelial-mesenchymal transition; ANOVA, analysis of variance.

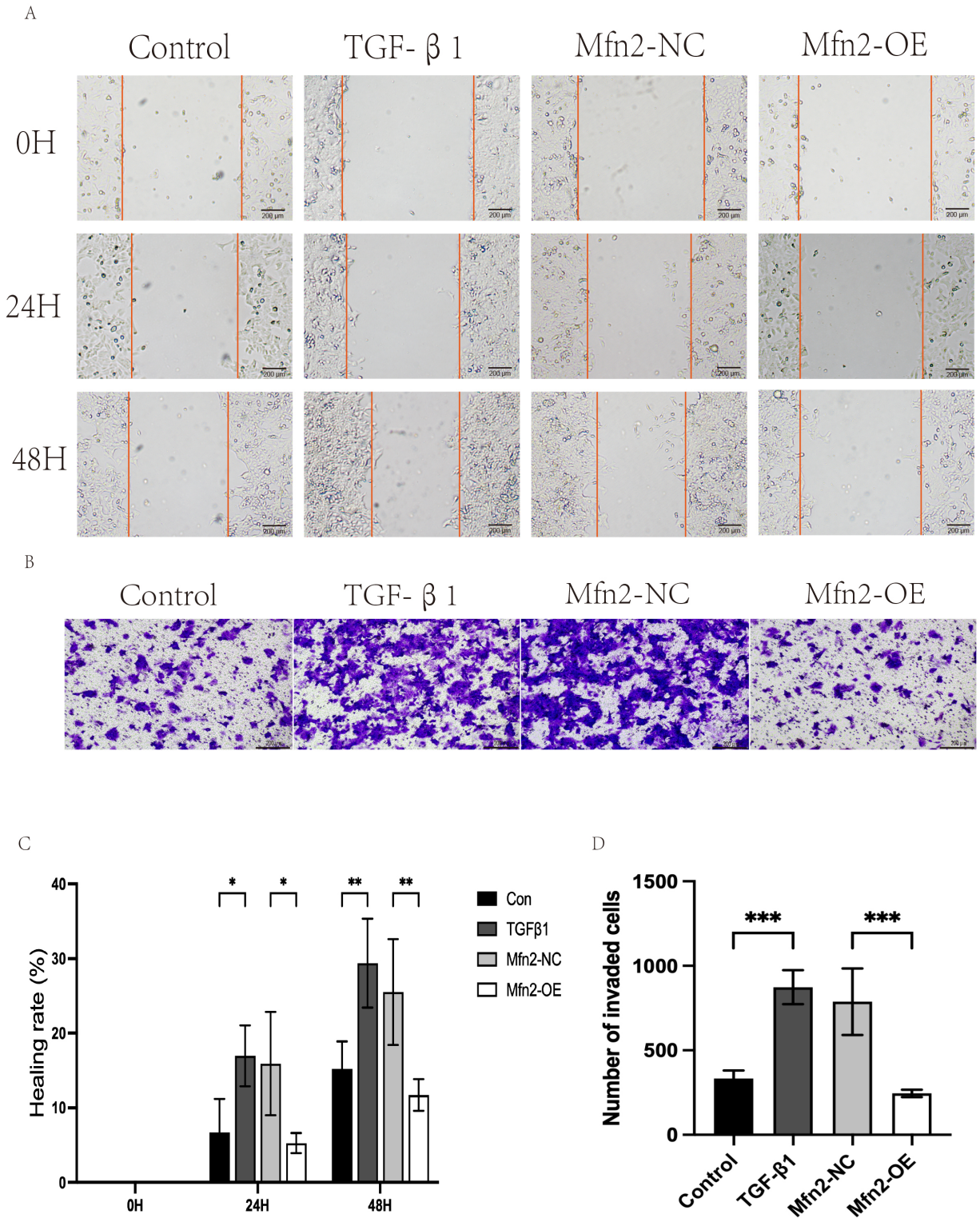

Fig. 3. Cell scratch assay and Transwell invasion assay. Functional verification: (A,C) cell scratch assay. Scale bar: 200 µm (×100). (B,D) Transwell invasion assay showed that EMT enhanced migration and invasion, while Mfn2 overexpression inhibited this effect. Scale bar: 200 µm (×100). Values represent mean ± SD, n = 3 (ANOVA). *$p < 0.05$, **$p < 0.01$, ***$p < 0.001$.

rectly leads to excessive mitochondrial fission (fragmentation) [13,23,24]. The morphological defect impairs mitochondrial electron transport chain (ETC) function, leading to the overproduction of ROS. Overproduced ROS act as key signaling molecules, activating nuclear factor kappa B (NF-κB) and hypoxia-inducible factor-1 alpha (HIF-1α) signaling pathways [6]. The activation of these pathways also induces the phosphorylation of the TGF-β/Smad path-

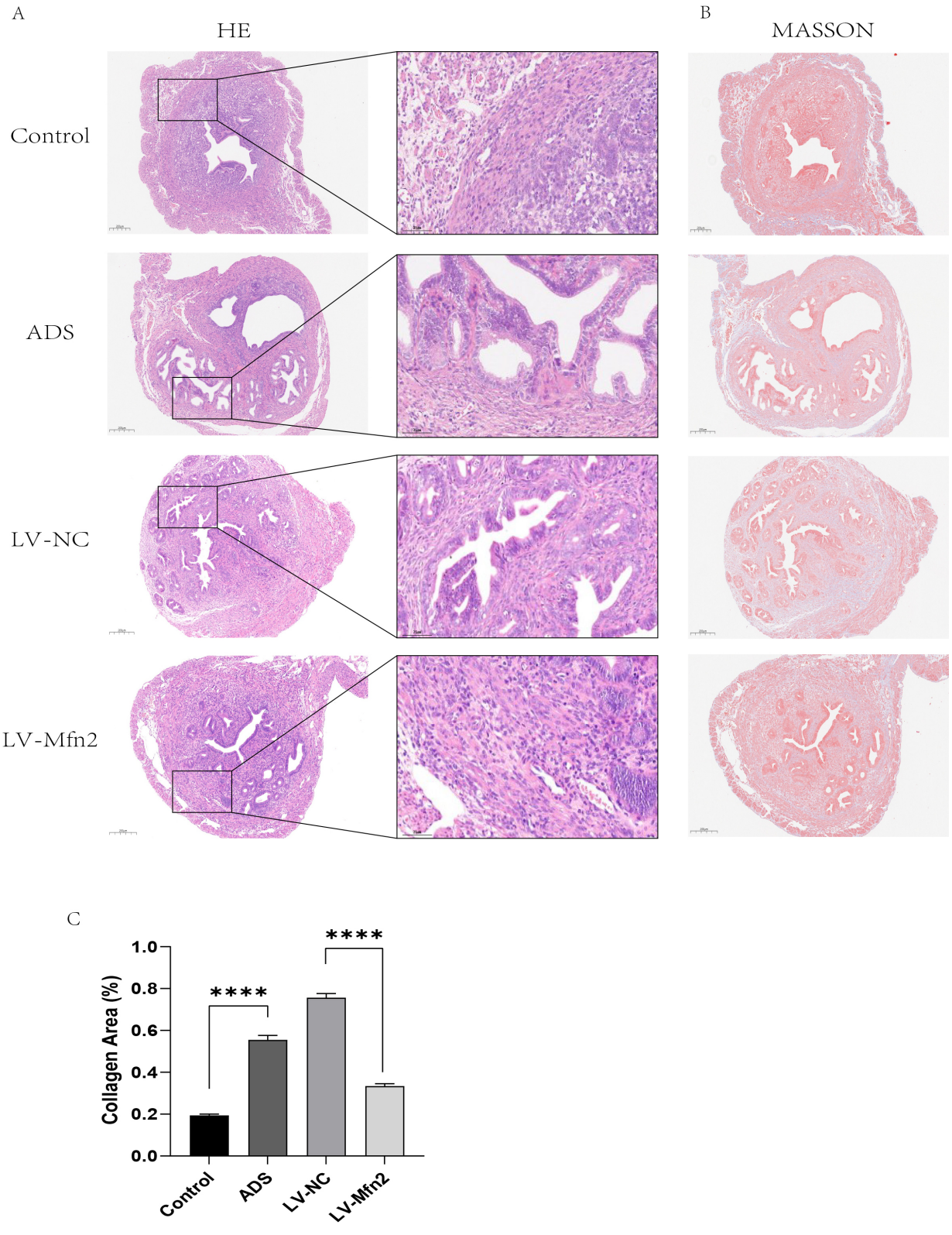

Fig. 4. Related pathological changes in mouse uterus. (A) H&E staining of the uterus of mice in each group: Control, adenomyosis model (ADS), Mfn2 negative control (LV-NC), lentiviral Mfn2 overexpression (LV-Mfn2). H&E staining showed the endometrial-myometrial junction. Scale bar: 200 μm (×60), 25 μm (×300). (B,C) Masson staining of the uterus in each group. Masson staining revealed the deposition of collagen fibers in the uterine tissue (in blue). The percentage of collagen area was quantitatively analyzed using the ImageJ software. Scale bar: 200 μm (×60). Values represent mean ± SD, n = 9 (ANOVA). ****$p < 0.0001$. H&E, hematoxylin and eosin.

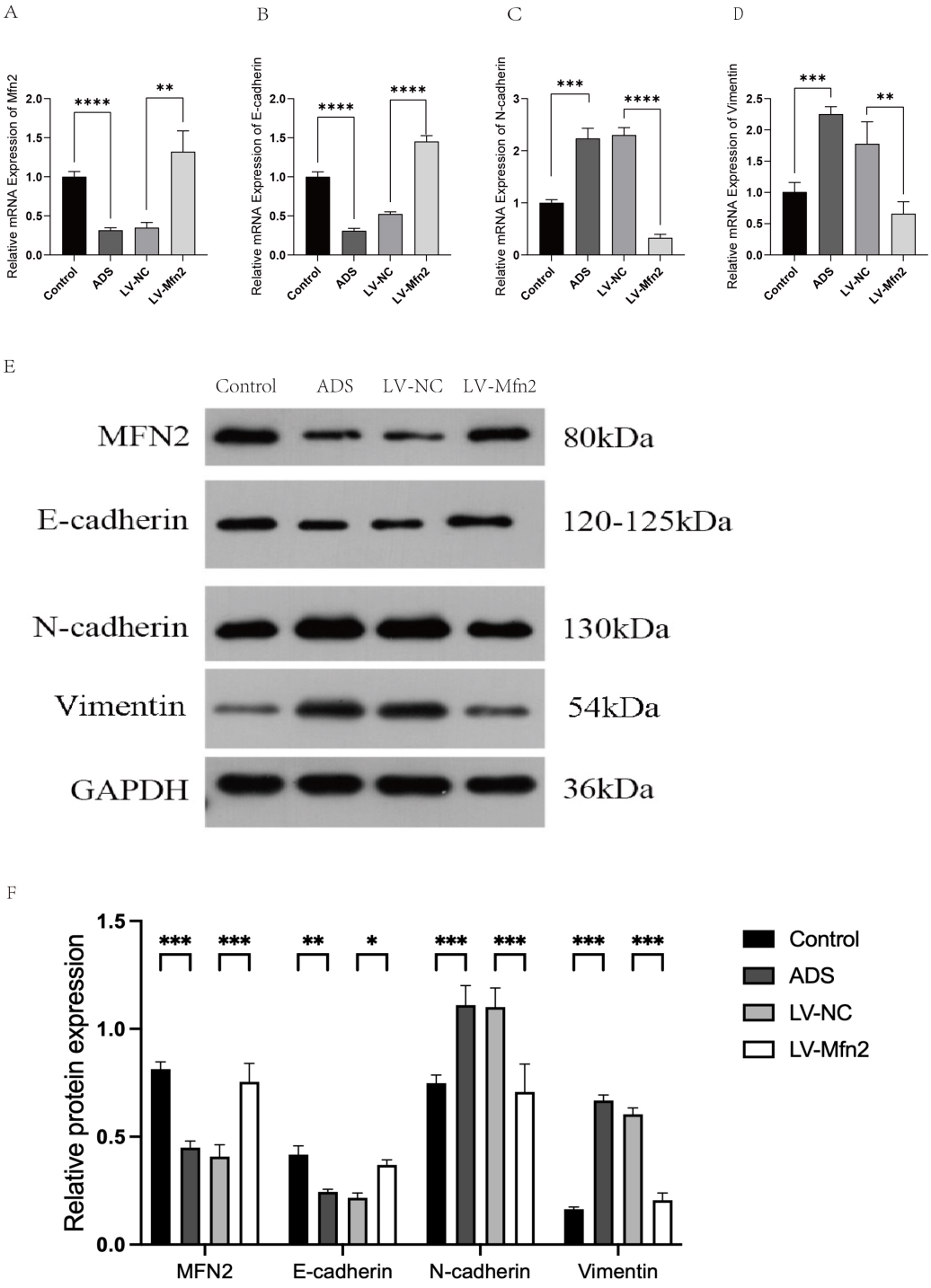

Fig. 5. Method validation of relevant markers in mouse uterus by qPCR and WB. (A–D) qPCR: the expression of E-cadherin, N-cadherin, Vimentin and Mfn2 mRNA in the uterus of the control vs model group (ADS) and Mfn2 negative control (LV-NC) vs Mfn2 overexpression group (LV-Mfn2). Values represent mean ± SD, n = 9 (*t*-test). (E,F) Western Blot was used to detect the protein expression of E-cadherin, N-cadherin, Vimentin and Mfn2 in the uterus of each group. Values represent mean ± SD, n = 9 (ANOVA). *$p < 0.05$, **$p < 0.01$, ***$p < 0.001$, ****$p < 0.0001$.

way, which eventually initiates the EMT process, which is manifested as the suppression of the expression of E-cadherin and the up-regulation of Vimentin and other mesenchymal markers.

2. Inhibition of metabolic reprogramming: Mitochondrial fragmentation not only leads to ROS accumulation (as described above), but also forces cells to forego efficient oxidative phosphorylation (OXPHOS) in favor of ineffi-

cient glycolysis (i.e., the Warburg effect) [25], a metabolic shift that is itself a hallmark feature of EMT. Overexpressed Mfn2 might restore the efficiency of OXPHOS by restoring the normal structure and function of mitochondrial cristae. At the same time, it is able to inhibit the activity of key glycolytic enzymes such as lactate dehydrogenase A (LDHA) [23,26], effectively opposing the aberrant metabolic adaptation that EMT depends on.

3. Regulation of mitochondrial-endoplasmic reticulum coupling: In addition to regulating mitochondrial fusion, Mfn2 is also involved in the formation and maintenance of mitochondrial-endoplasmic reticulum contact sites (MERCs), which are important for calcium (Ca^{2+}) signaling [27]. Calcium homeostasis disruption activates calcium-dependent proteases such as Calpain, which cleave E-cadherin and destabilize cell polarity, thereby inducing the EMT process. Therefore, Mfn2 could suppress the calpain-mediated EMT pathway through the stabilization of MERCs' integrity and calcium signaling.

The major finding of the present study—that Mfn2 overexpression substantially suppressed TGF-β1-induced EMT and cell invasion—provides important experimental validation of this hypothesis. Of course, the precise molecular network of Mfn2 regulating EMT is yet to be completely elucidated. Follow-up studies can track the effect of Mfn2 on ROS levels by knocking down Mfn2 or, more directly, quantify the OXPHOS/glycolytic flux alternation with the assistance of metabolomics technology to more comprehensively map the role of Mfn2.

In summary, this study demonstrates for the first time that Mfn2 plays a vital protective role in adenomyosis by inhibiting the process of EMT, which introduces new ideas for clinical diagnosis and treatment of adenomyosis. Studies have found that the low expression mode of Mfn2 in the endometrium of patients shows that Mfn2 can be used as an effective auxiliary diagnostic biomarker, and if combined with serum EMT markers (such as Vimentin), it is expected to significantly improve the accuracy of disease staging and invasiveness. In the therapeutic field, therapies targeting Mfn2 have shown broad prospects. Small-molecule compounds (e.g., natural product derivatives) with selective activation of Mfn2 can be developed through high-throughput screening and combined with in utero sustained release systems to achieve lesion-precise intervention. Lentiviral or adeno-associated virus (AAV) vector-mediated gene therapy has been shown to improve pathological phenotypes in animal models. Maximizing delivery efficiency or creating tissue-specific promoters may further improve efficacy and reduce toxicity in the future. Of particular interest is whether the combination of Mfn2 activators with existing antifibrotic treatments, e.g., gonadotrophin-releasing hormone (GnRH) agonists, can enhance efficacy through synergistic mechanisms. However, it is still necessary to systematically tackle key problems to facilitate clinical translation: to clarify the correlation of Mfn2 expression with clinical stage and symptom severity, to stringently evaluate the *in vivo* safety and off-target risk of Mfn2 agonists, and to fully explore the mechanisms of interaction between Mfn2 regulating mitochondrial function and Wnt/β-catenin and other key EMT pathways. Overcoming these challenges will accelerate the process of Mfn2 from bench to bedside and provide ever more accurate and efficient therapeutic approaches for patients with adenomyosis.

Limitations

Of course, we also know this study comes with several limitations that need to be addressed in the future. For one, the current clinical sample size is rather limited, and follow-up studies are urgently required to assess larger and more representative patient cohorts to more reliably validate the role of Mfn2 in adenomyosis and its clinical relevance. Although Ishikawa cells successfully mimic the TGF-β1-induced EMT phenotype, their tumor-derived properties are different from the benign lesion nature of adenomyosis, which may affect the physiological relevance of Mfn2 regulatory mechanisms, which needs to be further verified in primary adenomyosis cells or disease organoids, while studying non-EMT mechanisms will provide a comprehensive view of pathological mechanisms. At the same time, although tamoxifen-induced neonatal mouse model recapitulates the core pathological features of adenomyosis, the induction mechanism and anatomical structure are different from humans, which may limit the comparability of Mfn2 pathway regulation. In the future, the role of Mfn2 will be verified in larger human samples and the correlation between Mfn2 and clinical features of adenomyosis, such as disease stage and symptom severity, will be explored.

For another, although the function of Mfn2 and its relationship with EMT have been preliminarily revealed, the exact molecular mechanism of Mfn2 remains to be fully revealed. Gene knockout and RNA interference can be employed in the future to manipulate Mfn2 expression in cells and animal models with high accuracy, and their downstream effector molecules and signaling pathways can be further analyzed. In addition, since the regulatory network of Mfn2 is predicted to involve multiple signaling pathways and complex molecular interactions, multi-omics analysis (e.g., transcriptomics and proteomics) will be a promising direction to systemically reveal the key mechanism and network association of Mfn2. Overcoming these limitations will be of great value to clarify a deeper insight into the pathophysiology of adenomyosis and also provide a good foundation for the further exploration of Mfn2-targeted therapeutic strategies.

5. Conclusion

This study confirms that Mfn2 is a key repressor of adenomyosis progression. We consistently demonstrated that Mfn2 is significantly downregulated in human adenomyosis endometrium, in a cell model of EMT, and

in a mouse adenomyosis model. Functionally, restoring Mfn2 expression effectively reversed TGF-β1-induced EMT, suppressed endometrial cell migration and invasion *in vitro*, and, in a mouse model of adenomyosis, ameliorated key pathological features *in vivo*, including tissue invasion, fibrosis, and dysregulation of EMT markers. These results strongly suggest that Mfn2 plays a protective role in adenomyosis mainly by inhibiting the EMT process. Thus, Mfn2 holds promise as a novel diagnostic biomarker and therapeutic target for future interventions to mitigate this prevalent gynecologic disorder.

Availability of Data and Materials

The data supporting the results of this study are included in this paper and its online **Supplementary Material**.

Author Contributions

XW: Responsible for the conceptualization and design of this study, and experimented. NNX: Responsible for writing the first draft of the manuscript and improving the study design. XQ: assisted in the H&E staining of histological samples, immunohistochemical staining, and the scoring of their results. QH and CD: participated in the execution of cell culture, animal model establishment, and tissue sampling. HY: supervised the whole research process, guided the implementation of the study, and analyzed and interpreted the data. All authors contributed to editorial changes in the manuscript. All authors read and approved the final manuscript. All authors have participated sufficiently in the work and agreed to be accountable for all aspects of the work.

Ethics Approval and Consent to Participate

The Ethics Committee of Yichang Central People's Hospital approved this human subject/tissue sample study (Approval No. [2024-252-01]). All subjects gave written informed consent in compliance with the Declaration of Helsinki. Anonymity and confidentiality of the patients were strictly maintained during the study. All animal procedures were conducted according to the ARRIVE Guidelines for the Care and Use of Laboratory Animals and were endorsed by the Experimental Animal Ethics Committee of China Three Gorges University (Protocol No. [2024070I]). All animal experiments complied with ethical guidelines and the principles of Replacement, Reduction, and Refinement (3Rs). Efforts were made to minimize animal suffering, including the use of anesthesia during surgical procedures and the application of humane endpoints for euthanasia.

Acknowledgment

This study was strongly supported by the Central Laboratory of Wujia Branch of Yichang Central People's Hospital in terms of research sites and equipment, which is greatly appreciated. At the same time, we sincerely thank the Laboratory Animal Center of China Three Gorges University for providing professional assistance in the feeding and management of laboratory animals and the technical operation of gavage.

Funding

This study was supported by the Natural Science Foundation of Hubei Province (Joint Fund Project: 2024AFD189).

Conflict of Interest

The authors declare no conflict of interest.

Supplementary Material

Supplementary material associated with this article can be found, in the online version, at https://doi.org/10.31083/CEOG46464.

References

[1] Kolovos G, Dedes I, Imboden S, Mueller M. Adenomyosis-A Call for Awareness, Early Detection, and Effective Treatment Strategies: A Narrative Review. Healthcare (Basel, Switzerland). 2024; 12: 1641. https://doi.org/10.3390/healthcare12161641.

[2] Struble J, Reid S, Bedaiwy MA. Adenomyosis: A Clinical Review of a Challenging Gynecologic Condition. Journal of Minimally Invasive Gynecology. 2016; 23: 164–185. https://doi.org/10.1016/j.jmig.2015.09.018.

[3] Vannuccini S, Luisi S, Tosti C, Sorbi F, Petraglia F. Role of medical therapy in the management of uterine adenomyosis. Fertility and Sterility. 2018; 109: 398–405. https://doi.org/10.1016/j.fertnstert.2018.01.013.

[4] Chapron C, Vannuccini S, Santulli P, Abrão MS, Carmona F, Fraser IS, *et al*. Diagnosing adenomyosis: an integrated clinical and imaging approach. Human Reproduction Update. 2020; 26: 392–411. https://doi.org/10.1093/humupd/dmz049.

[5] Chen D, Qiao H, Wang Y, Ling Zhou, Yin N, Fang L, *et al*. Adenomyosis-derived extracellular vesicles endow endometrial epithelial cells with an invasive phenotype through epithelial-mesenchymal transition. Genes & Diseases. 2020; 7: 636–648. https://doi.org/10.1016/j.gendis.2020.01.011.

[6] Marconi GD, Fonticoli L, Rajan TS, Pierdomenico SD, Trubiani O, Pizzicannella J, *et al*. Epithelial-Mesenchymal Transition (EMT): The Type-2 EMT in Wound Healing, Tissue Regeneration and Organ Fibrosis. Cells. 2021; 10: 1587. https://doi.org/10.3390/cells10071587.

[7] Youssef KK, Narwade N, Arcas A, Marquez-Galera A, Jiménez-Castaño R, Lopez-Blau C, *et al*. Two distinct epithelial-to-mesenchymal transition programs control invasion and inflammation in segregated tumor cell populations. Nature Cancer. 2024; 5: 1660–1680. https://doi.org/10.1038/s43018-024-00839-5.

[8] Stratopoulou CA, Cussac S, d'Argent M, Donnez J, Dolmans MM. M2 macrophages enhance endometrial cell invasiveness by promoting collective cell migration in uterine adenomyosis. Reproductive Biomedicine Online. 2023; 46: 729–738. https://doi.org/10.1016/j.rbmo.2023.01.001.

[9] Naón D, Hernández-Alvarez MI, Shinjo S, Wieczor M, Ivanova S, Martins de Brito O, *et al*. Splice variants of mitofusin 2 shape

the endoplasmic reticulum and tether it to mitochondria. Science (New York, N.Y.). 2023; 380: eadh9351. https://doi.org/10.1126/science.adh9351.

[10] Joaquim M, Altin S, Bulimaga MB, Simões T, Nolte H, Bader V, *et al*. Mitofusin 2 displays fusion-independent roles in proteostasis surveillance. Nature Communications. 2025; 16: 1501. https://doi.org/10.1038/s41467-025-56673-5.

[11] Kolitsida P, Saha A, Caliri A, Assali E, Riera AM, Itskanov S, *et al*. Mfn2 induces NCLX-mediated calcium release from mitochondria. bioRxiv. 2024. (preprint)

[12] Inagaki S, Suzuki Y, Kawasaki K, Kondo R, Imaizumi Y, Yamamura H. Mitofusin 1 and 2 differentially regulate mitochondrial function underlying Ca^{2+} signaling and proliferation in rat aortic smooth muscle cells. Biochemical and Biophysical Research Communications. 2023; 645: 137–146. https://doi.org/10.1016/j.bbrc.2023.01.044.

[13] Filadi R, Pendin D, Pizzo P. Mitofusin 2: from functions to disease. Cell Death & Disease. 2018; 9: 330. https://doi.org/10.1038/s41419-017-0023-6.

[14] Yang K, Hu HY, Zhang J, Yan YS, Chen WQ, Liu Y, *et al*. Metabolic and biophysical study of the $MFN2^{Ile213Thr}$ mutant causing Hereditary Motor and Sensory Neuropathy (HMSN). American Journal of Translational Research. 2021; 13: 11501–11512.

[15] Sun D, Zhu H, Ai L, Wu H, Wu Y, Jin J. Mitochondrial fusion protein 2 regulates endoplasmic reticulum stress in preeclampsia. Journal of Zhejiang University. Science. B. 2021; 22: 165–170. https://doi.org/10.1631/jzus.B2000557.

[16] Ahn SY. Mitofusin-2 enhances cervical cancer progression through Wnt/β-catenin signaling. BMB Reports. 2024; 57: 194–199. https://doi.org/10.5483/BMBRep.2023-0205.

[17] Yan L, Luo X, Hang C, YuWang, Zhang Z, Xu S, *et al*. Unraveling the Mfn2-Warburg effect nexus: a therapeutic strategy to combat pulmonary arterial hypertension arising from catch-up growth after IUGR. Respiratory Research. 2024; 25: 328. https://doi.org/10.1186/s12931-024-02957-1.

[18] You MH, Jeon MJ, Kim SR, Lee WK, Cheng SY, Jang G, *et al*. Mitofusin-2 modulates the epithelial to mesenchymal transition in thyroid cancer progression. Scientific Reports. 2021; 11: 2054. https://doi.org/10.1038/s41598-021-81469-0.

[19] Ashraf R, Kumar S. Mfn2-mediated mitochondrial fusion promotes autophagy and suppresses ovarian cancer progression by reducing ROS through AMPK/mTOR/ERK signaling. Cellular and Molecular Life Sciences: CMLS. 2022; 79: 573. https://doi.org/10.1007/s00018-022-04595-6.

[20] Li P, Wang ZQ, Zhao LJ, Li XP, Wang JL. Transforming growth factor-β induces epithelial–mesenchymal transition in endometrial carcinoma cells. Zhonghua Fu Chan Ke Za Zhi. 2014; 49: 628–630. https://doi.org/10.3760/cma.j.issn.0529-567x.2014.08.016. (In Chinese)

[21] Shi YX, Xu L, Wang X, Zhang KK, Zhang CY, Liu HY, *et al*. Paris polyphylla ethanol extract and polyphyllin I ameliorate adenomyosis by inhibiting epithelial-mesenchymal transition. Phytomedicine: International Journal of Phytotherapy and Phytopharmacology. 2024; 127: 155461. https://doi.org/10.1016/j.phymed.2024.155461.

[22] Yuan B, Wang W, Zhao H, Wang L. Role of lncRNA TUG1 in Adenomyosis and its Regulatory Mechanism in Endometrial Epithelial Cell Functions. Endocrinology. 2022; 163: bqac033. https://doi.org/10.1210/endocr/bqac033.

[23] Zanfardino P, Amati A, Perrone M, Petruzzella V. The Balance of MFN2 and OPA1 in Mitochondrial Dynamics, Cellular Homeostasis, and Disease. Biomolecules. 2025; 15: 433. https://doi.org/10.3390/biom15030433.

[24] Jiang S, Nandy P, Wang W, Ma X, Hsia J, Wang C, *et al*. Mfn2 ablation causes an oxidative stress response and eventual neuronal death in the hippocampus and cortex. Molecular Neurodegeneration. 2018; 13: 5. https://doi.org/10.1186/s13024-018-0238-8.

[25] Delgado ME, Cárdenas BI, Farran N, Fernandez M. Metabolic Reprogramming of Liver Fibrosis. Cells. 2021; 10: 3604. https://doi.org/10.3390/cells10123604.

[26] Yao CH, Wang R, Wang Y, Kung CP, Weber JD, Patti GJ. Mitochondrial fusion supports increased oxidative phosphorylation during cell proliferation. eLife. 2019; 8: e41351. https://doi.org/10.7554/eLife.41351.

[27] Liu X, Li T, Tu X, Xu M, Wang J. Mitochondrial fission and fusion in neurodegenerative diseases: Ca^{2+} signalling. Molecular and Cellular Neurosciences. 2025; 132: 103992. https://doi.org/10.1016/j.mcn.2025.103992.